Support information

Solvatochromic Behavior of a Nanotubular Metal-Organic Framework for Sensing Small Molecules

*Zhen-Zhong Lu Rui Zhang Yi-Zhi Li Zi-Jian Guo He-Gen Zheng**

State Key Laboratory of Coordination Chemistry, School of Chemistry and Chemical Engineering, National Laboratory of Microstructures, Nanjing University, Nanjing 210093 (P.R. China)
Fax: (+86)25-83314502, E-mail: zhenghg@nju.edu.cn

1. Materials and methods

$(NH_4)_2WS_4$ and dptz ligand was synthesized according to reported procedures.[S1] Other chemicals were obtained from commercial sources and used as received.

Single-crystal X-ray crystallographic studies. Data were collected on a Bruker-AXS APEXII X-ray diffractometer at 291 K. Raw data collection and refinement were done using SMART. Data reduction was performed using SAINT+ and data were corrected for Lorentz and polarization effects.[S2] The structures were solved by direct methods and refined by full matrix least-squares on F^2 using the SHELXTL software package. Non-hydrogen atoms were refined with anisotropic displacement parameters during the final cycles. Hydrogen atoms of ligands were calculated in ideal positions with isotropic displacement parameters. The solvent molecules in the structure were found to be highly disordered and were impossible to refine using conventional discrete-atom models. The diffuse electron densities resulting from the residual solvent molecules were removed from the data set using the SQUEEZE routine of PLATON and refined further using the data generated.[S3] The final formula of **1** was determined from the SQUEEZE results combined with elemental analysis, IR and TGA data. The diffuse electron densities in the nanotubes of the desolvated crystal **1′** revealed by PLATON are found to be 1/7 of those in the as synthesized sample **1**⊃DMF.

The IR spectra were obtained as KBr pellets on a VECTOR 22 spectrometer. TGA measurements were conducted on a TA-SDT 2960 with a heating rate of 10 $^oC\ min^{-1}$ under a flux of nitrogen. The powder X-ray diffraction analysis was performed by a Philips X-pert X-ray diffractometer at a scanning rate of 4° min^{-1} in the 2θ range from 5° to 60° with graphite monochromatized Cu Kα radiation (λ = 1.5418 Å).

UV-vis spectra were collected on a UV-3600 spectrophotometer working in diffuse reflectance mode. The Kubelka-Munk equation was used to calculate absorption at the various wavelengths. Using the absorption versus energy plot, the first derivative of the absorption spectrum equation was calculated, and the inversion points were identified as band gaps.[S4]

2. Synthesis procedures

2.1 Synthesis of $\{[(WS_4Cu_4)I_2(dptz)_3]\cdot DMF\}_n$ 1⊃DMF

10.0 mL DMF contains a mixture of $(NH_4)_2WS_4$ (0.01 mmol), CuI (0.04 mmol) and Et_4NI (0.01 mmol) was stirred for 10 minutes under a nitrogen atmosphere. 3.0 mL filtrate was layered on top of 4.0 mL nitrobenzene containing dptz (0.01 mmol) in a test tube. The test tube was sealed and allowed to stand at room temperature. Dark red crystals were collected in a month (yield: ~60 % based on ligand). Elemental analysis (%) for **1**⊃DMF $C_{39}H_{31}N_{19}OI_2WS_4Cu_4$: calcd C 29.24, H 1.95, N 16.61; found C 30.06, H 2.01, N 16.73.

2.2 Synthesis of desolvated sample 1′

Crystals of **1**⊃DMF were immersed in methanol for 3 days. The solvent was exchanged with fresh methanol every 12 hours. The methanol exchanged crystals **1**⊃CH_3OH were collected by filtration. The desolvated compound **1′** was obtained by heating **1**⊃CH_3OH at 60 °C under vacuum for 10 hours.

2.3 Synthesis of inclusion compounds 1⊃solvent

Immersing the as-made sample **1**⊃DMF in different solvent. Change fresh solvent every 12 hours, the inclusion compounds **1**⊃solvent were obtained after 3 days.

2.4 Synthesis of inclusion compounds 2⊃solvent

Immersing the sample **2**⊃DMF in different solvent. Change fresh solvent every 12 hours, the inclusion compounds **2**⊃solvent were obtained after 3 days.

3. Supporting tables and figures

Table S1. C–H···N hydrogen bonds distances and angles in **1** and **1′** (Å, °).

1				**1′**			
D–H···A	d(H···A)	d(D···A)	∠(DHA)	D–H···A	d(H···A)	d(D···A)	∠(DHA)
$C_{10}'–H_{10}'\cdots N_5'$	2.480(1)	3.214(2)	136.0(2)	$C_{11}'–H_{11}'\cdots N_5'$	2.606(1)	3.346(2)	136.8(1)
$C_9'–H_9'\cdots N_4'$	2.643(2)	3.294(2)	127.6(1)	$C_{12}'–H_{12}'\cdots N_4'$	2.725(2)	3.316(3)	122.3(2)
$C_4'–H_4'\cdots N_2'$	2.796(3)	3.365(3)	129.7(1)	$C_2'–H_2'\cdots N_2'$	2.874(1)	3.450(2)	121.4(2)

Table S2. Band gaps of different inclusion compounds and Reichardt's solvent polarity parameters E_T^N.

Solvent	Band gap	E_T^N	Solvent	Band gap	E_T^N
CH_3CN	2.04	0.460	H_2O	1.93	1.000
DMF	1.77	0.386	CH_3OH	1.82	0.762
Acetone	1.72	0.355	C_2H_5OH	1.71	0.654
$CHCl_3$	1.43	0.259	1,4-dioxane	—	0.164

Table S3. Crystal and structure refinement data for compound **1** and **1′.**

	1	**1′**
Empirical formula	$C_{36}H_{24}I_2Cu_4N_{18}S_4W$	$C_{36}H_{24}Cu_4I_2N_{18}S_4W$
Temperature	291	291
MoKa,	0.71073	0.71073
Crystal system	Orthorhombic	Orthorhombic
Space group	*Ccca*	*Ccca*
a, Å	26.589(7)	26.860(6)
b, Å	31.767(8)	31.492(7)
c, Å	13.739(3)	13.905(5)
a (°)	90.00	90.00
β (°)	90.00	90.00
γ (°)	90.00	90.00
V, Å^3	11604(5)	11762(6)
Z	8	8
ρ_{calc} Mg/m^3	1.750	1.727
μ, mm^{-1}	4.666	4.604
Refl. collected	29583	27991
Independent refl.	5721/4400	5215/3712
Final R indices(R1)	0.0490	0.0636
[I>2σ(I)] wR2	0.1223	0.1581
R indices	0.0729	0.0839
(all data) wR2	0.1298	0.1676
GOOF	1.038	1.036

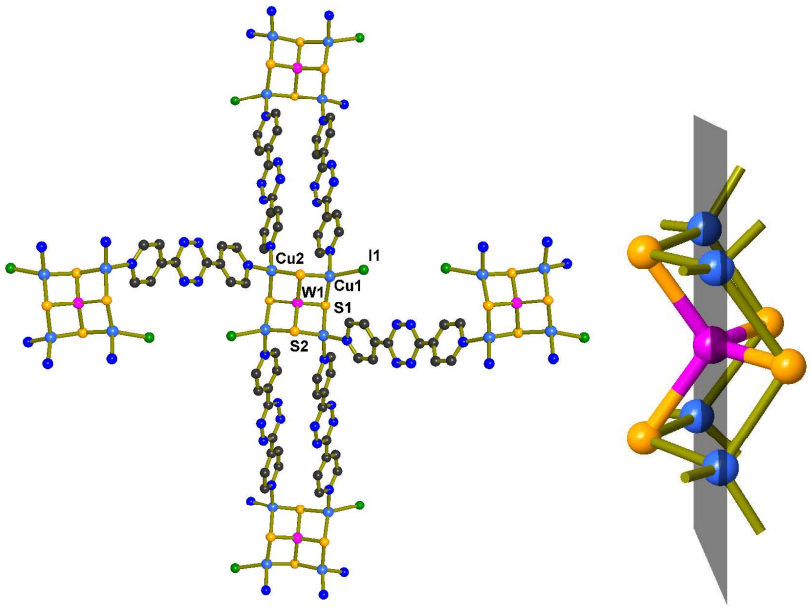

(a) (b)

Figure S1. (a) Coordination environment of the $WS_4Cu_4^{2+}$ cluster unit [W1···Cu1 = 2.707(2) Å, W1···Cu2 = 2.688(3) Å, □W···W···W = 99.21(1) ~ 119.32(2)°]. (b) Side view of the saddle-shaped cluster unit with the four Cu and the W atom in one plane

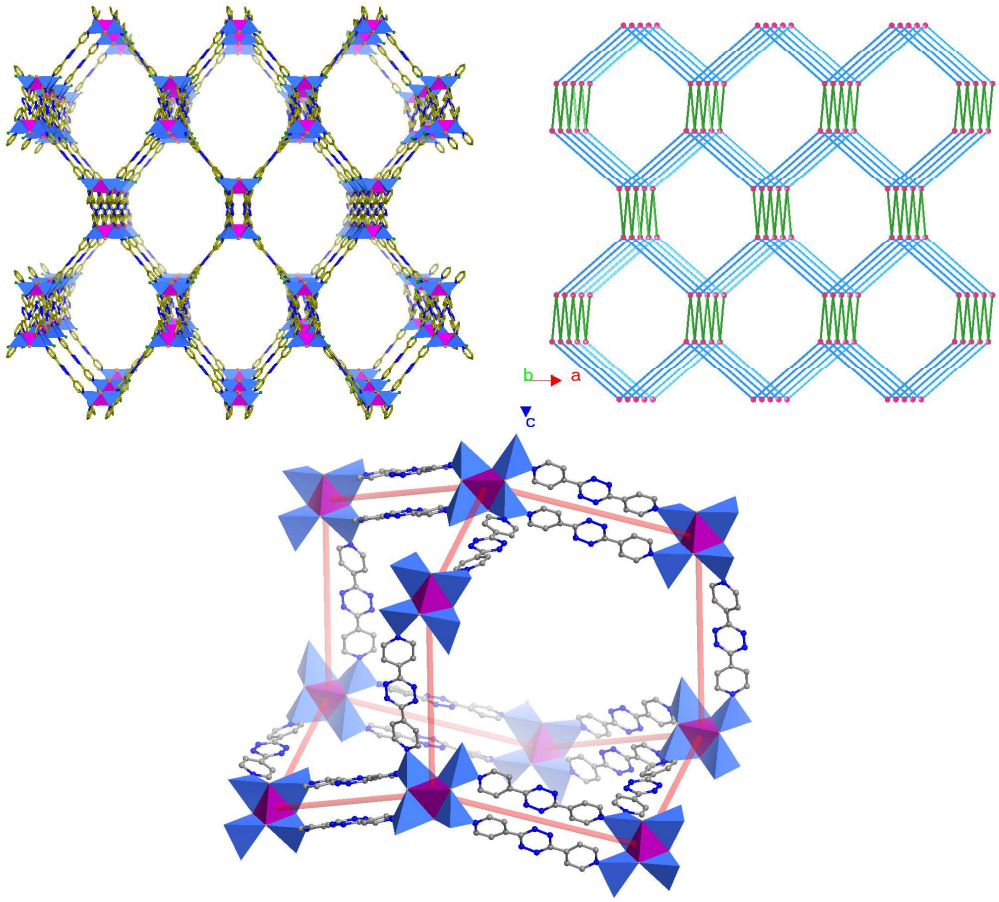

Figure S2. The diamondoid networks and adamantane cage of **1**.

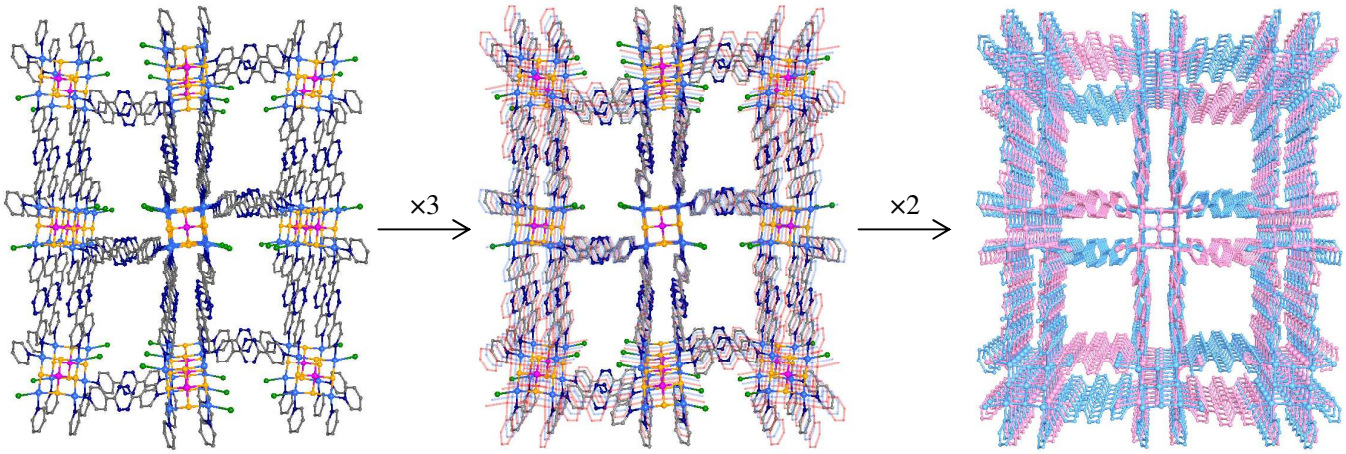

Figure S3. A presentation demonstrates the interpenetration mode of **1**. (a) One diamondoid network of **1** seeing along the *c* direction. (b) The three networks interpenetrating by the cell-translation along the *c* direction. (c) The over six networks containing two sets of 3-fold diamondoid networks, which are related by the *C*-centering translation.

3. PXRD, UV-vis, IR, TGA and photographs

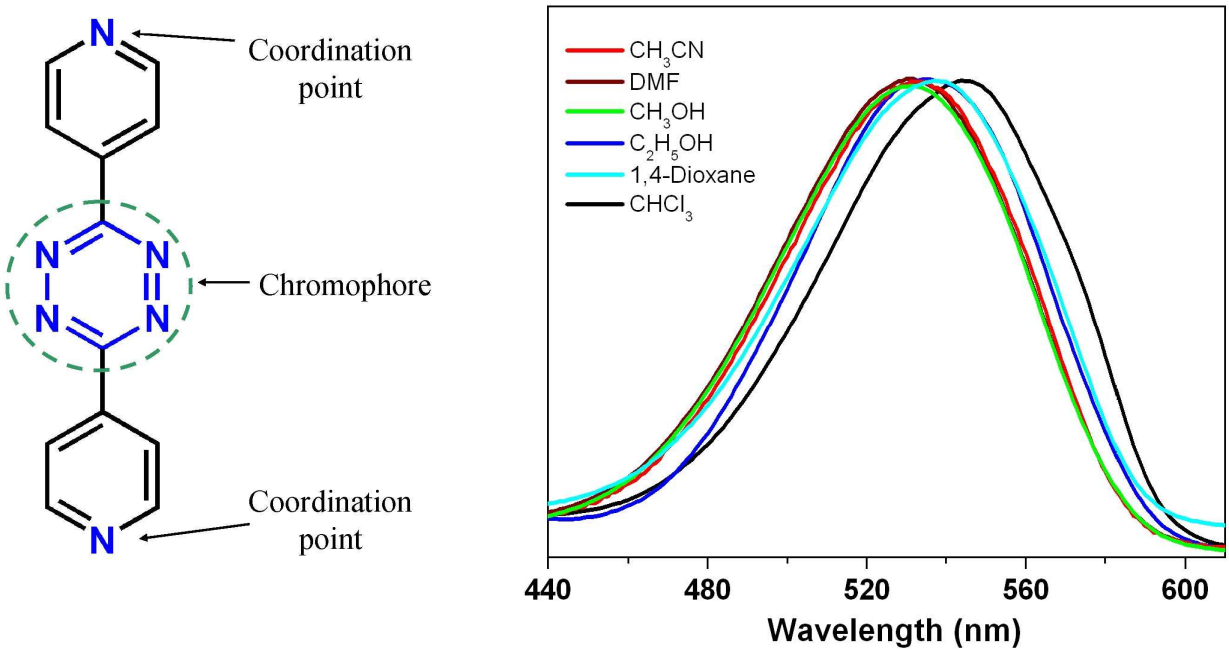

Figure S4 UV-vis absorption spectra of dptz ligand in different solvent.

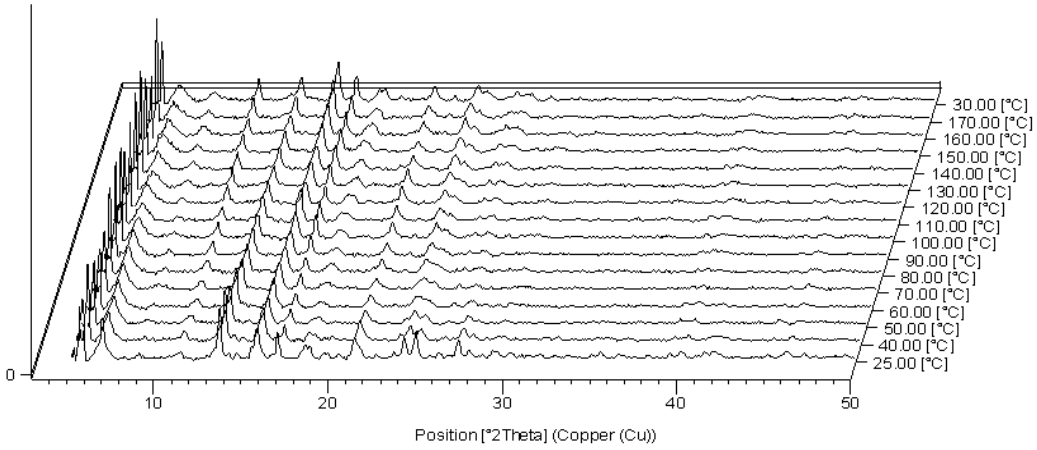

Figure S5. Powder X-ray thermo-diffraction of as-made **1**⊃DMF.

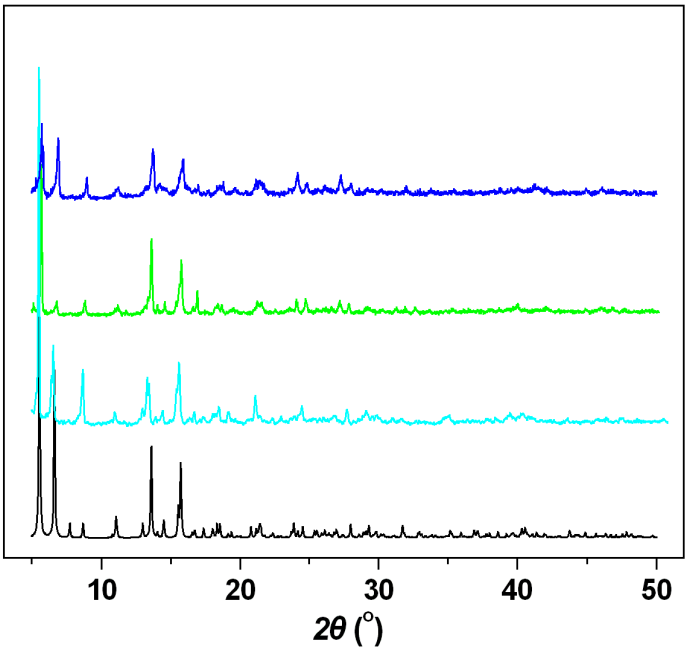

Figure S6. PXRD of stimulated **1**⊃DMF (black), as-made **1**⊃DMF (cyan), **1**⊃CH_3CN (green) and **1**⊃$CHCl_3$ (blue).

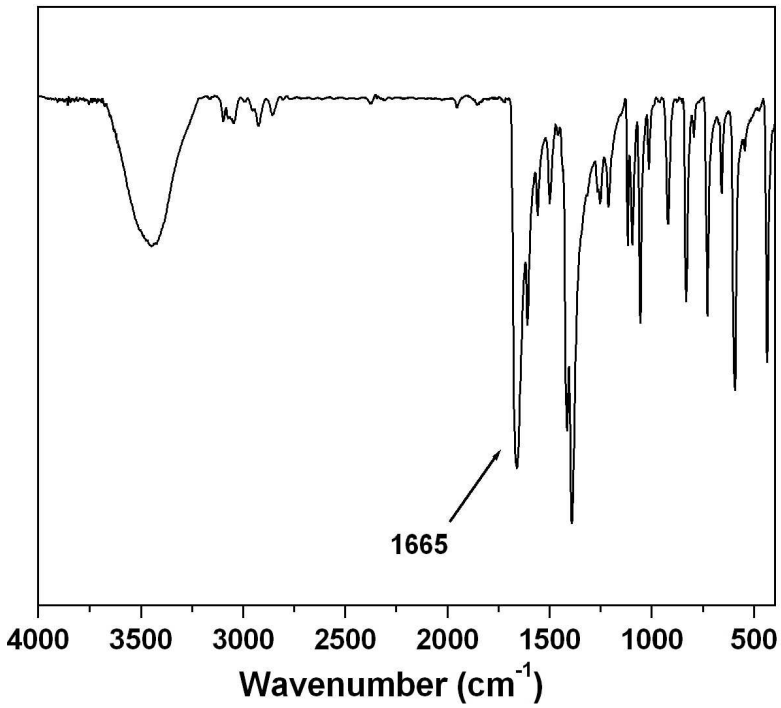

Figure S7. IR spectra of as-made sample **1⊃DMF**

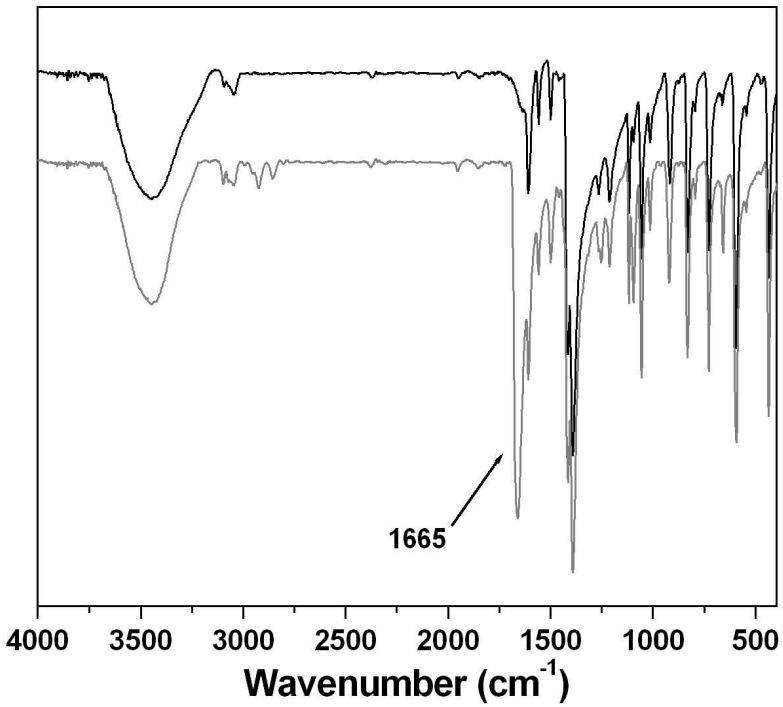

Figure S8. IR spectra of **1⊃CH_3OH** (black) and **1**⊃DMF (gray), the disappearance of the strong peak at 1665 (the C=O stretching peak of DMF) indicates the exchanging of DMF with CH_3OH.

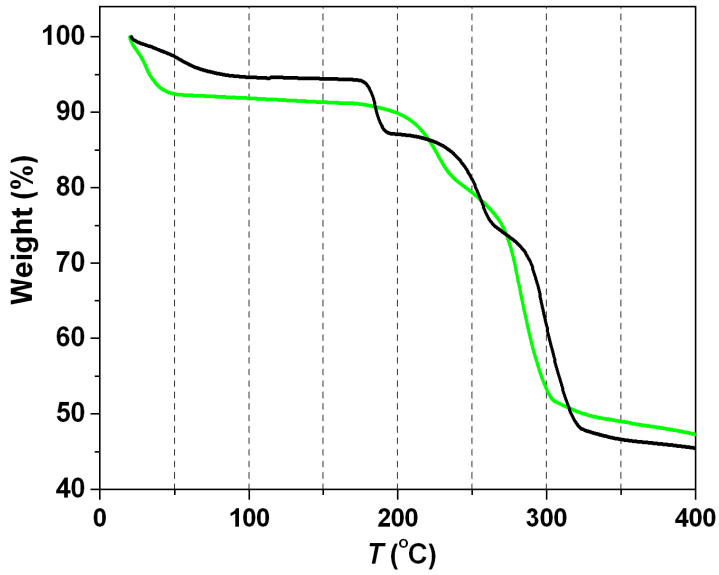

Figure S9. TG of **1**⊃DMF (black) and **1**⊃CH_3OH (green). Removal of DMF needs much higher temperature (~ 100 °C) than removal of CH_3OH (< 60 °C) from the framework.

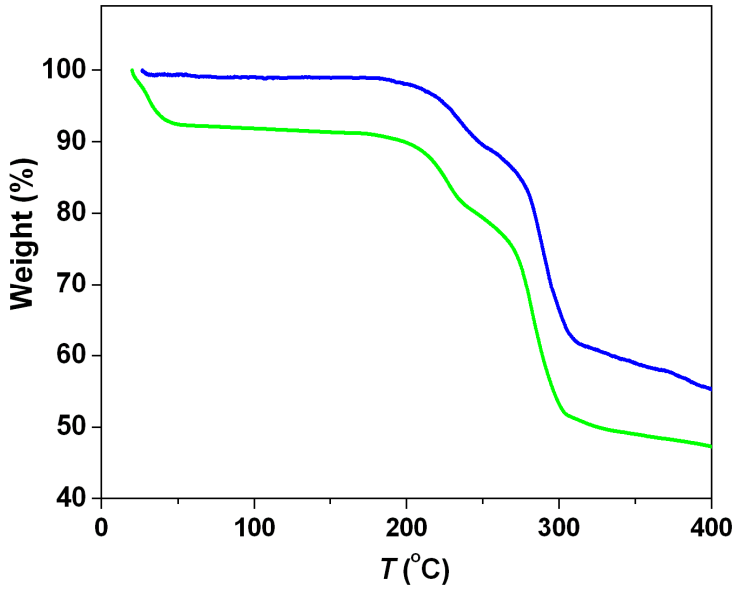

Figure S10. TG of **1**⊃CH_3OH (green) and desolvated sample **1′** (blue).

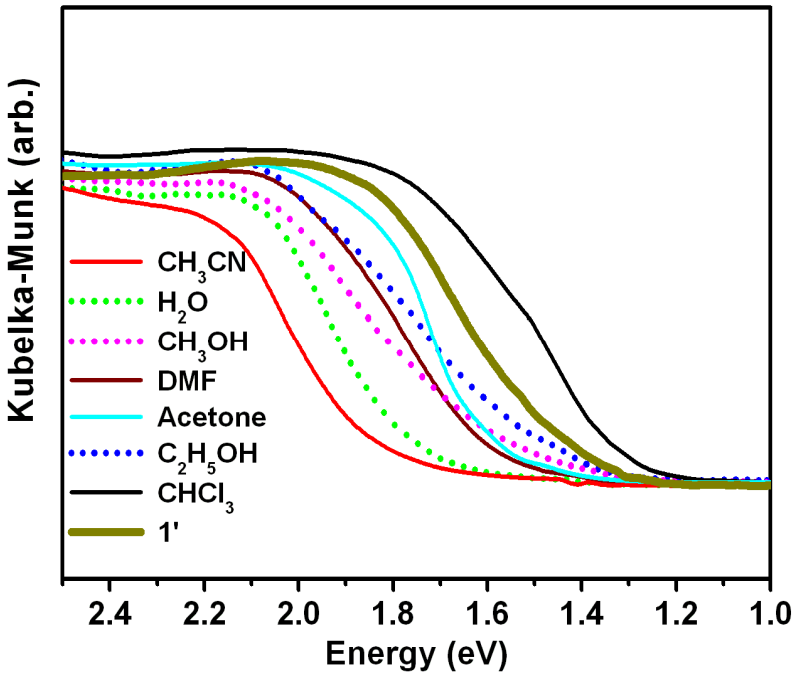

Figure S11. The UV-vis spectra of inclusion compounds **1**⊃solvent and desolvated sample **1′**.

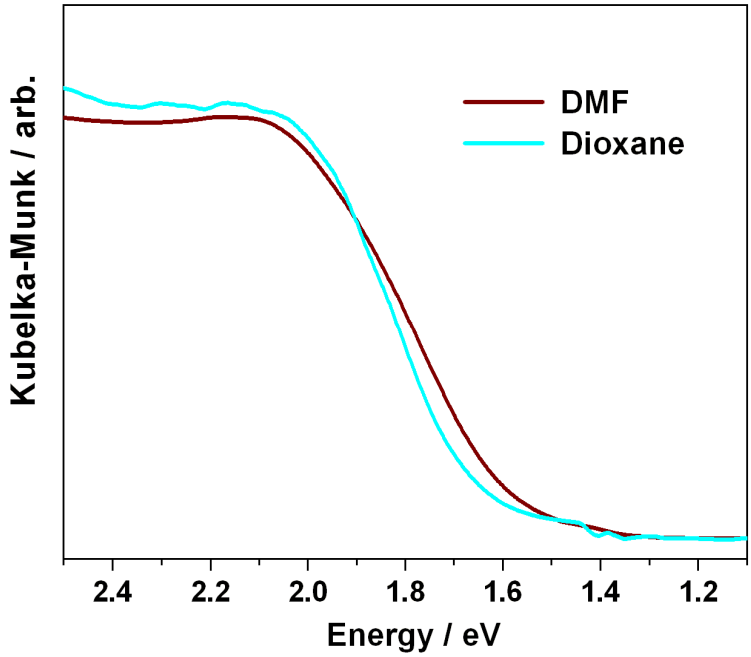

Figure S12. The UV-vis spectra of **1**⊃DMF and the sample obtained by immersing **1**⊃DMF in 1,4-dioxane for 5 days.

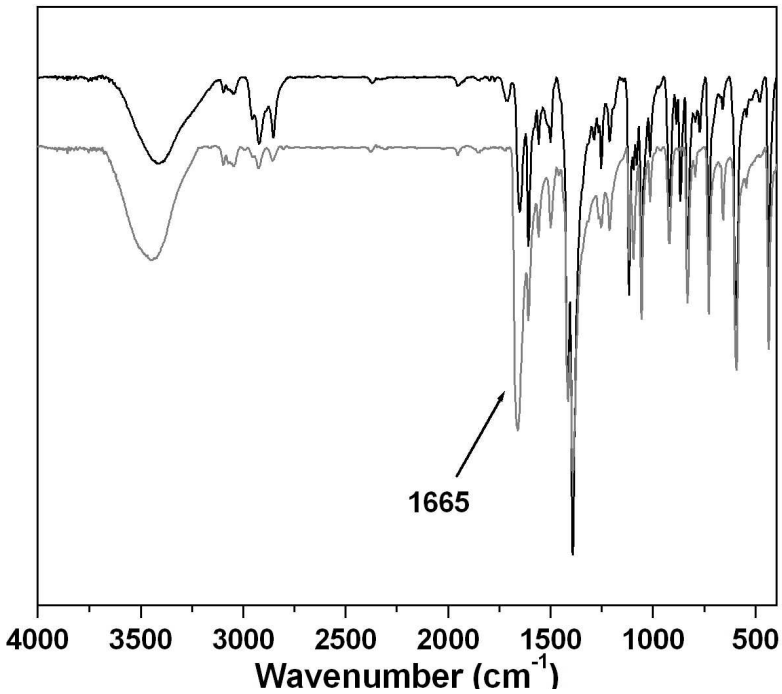

Figure S13. IR spectra of the sample obtained by immersing **1**⊃DMF in **1,4-dioxane** for 5 days (black) and **1**⊃DMF (gray), the strong peak at 1665 (the C=O stretching peak of DMF) indicates nearly no exchanging of DMF with 1,4-dioxane.

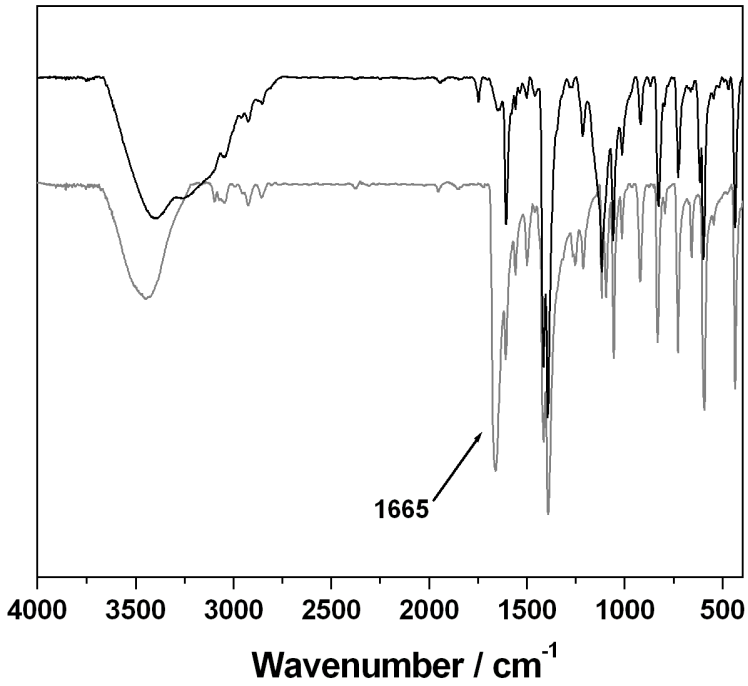

Figure S14. IR spectra of **1**⊃**CH_3CN** (black) and **1**⊃DMF (gray), the sharply decrease of the strong peak at 1665 (the C=O stretching peak of DMF) indicates the exchanging of DMF with CH_3CN.

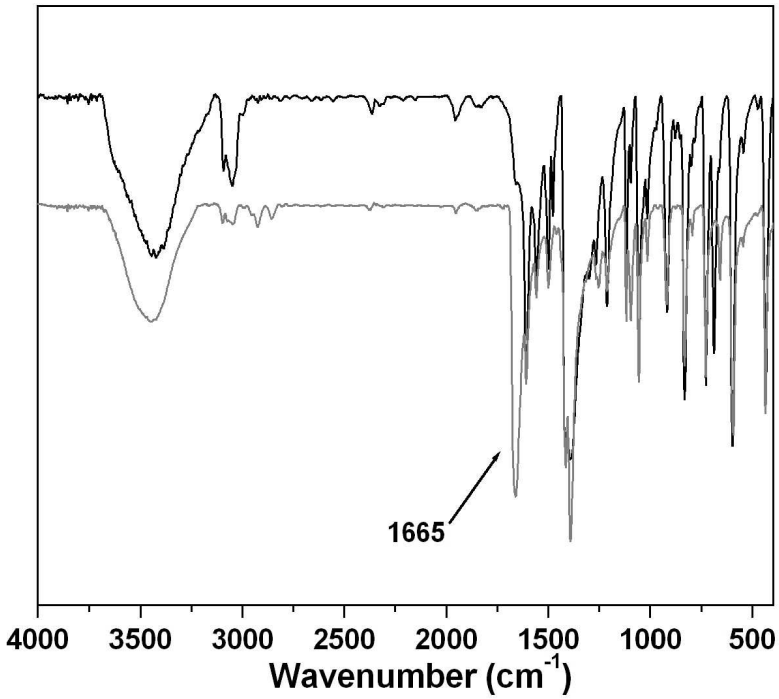

Figure S15. IR spectra of **1⊃CHCl$_3$** (black) and **1**⊃DMF (gray), the sharply decrease of the strong peak at 1665 (the C=O stretching peak of DMF) indicates the exchanging of DMF with $CHCl_3$.

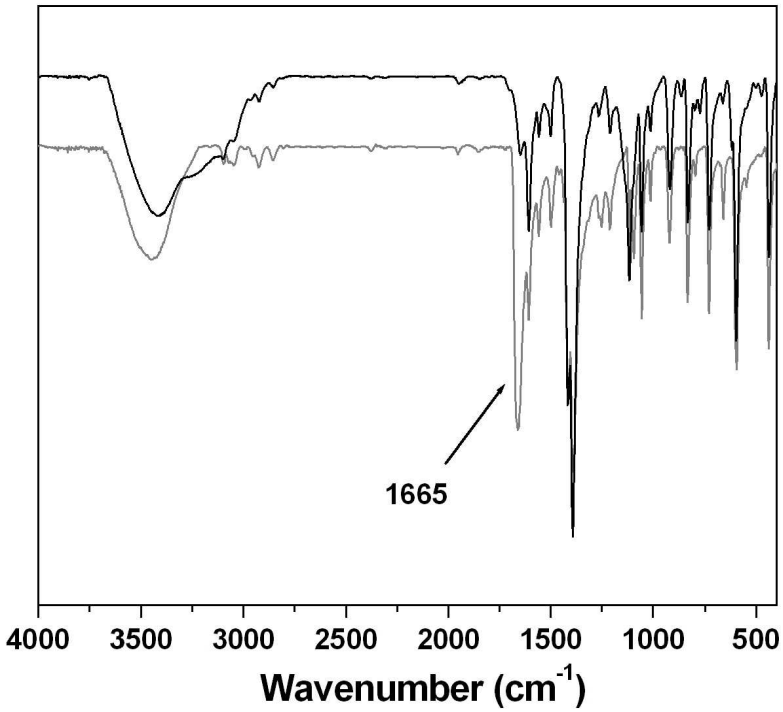

Figure S16. IR spectra of **1⊃C$_2$H$_5$OH** (black) and **1**⊃DMF (gray), the sharply decrease of the strong peak at 1665 (the C=O stretching peak of DMF) indicates the exchanging of DMF with C_2H_5OH.

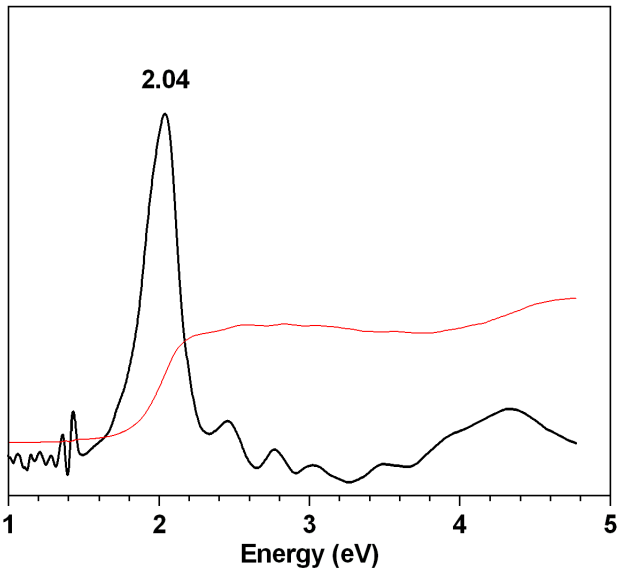

Figure S17. The Kubelka-Munk equation transformed UV-Vis absorption of **1⊃CH$_3$CN** (red line). The first derivative of the absorption spectrum equation was calculated (black line), and the inversion points were identified as 2.04 eV.

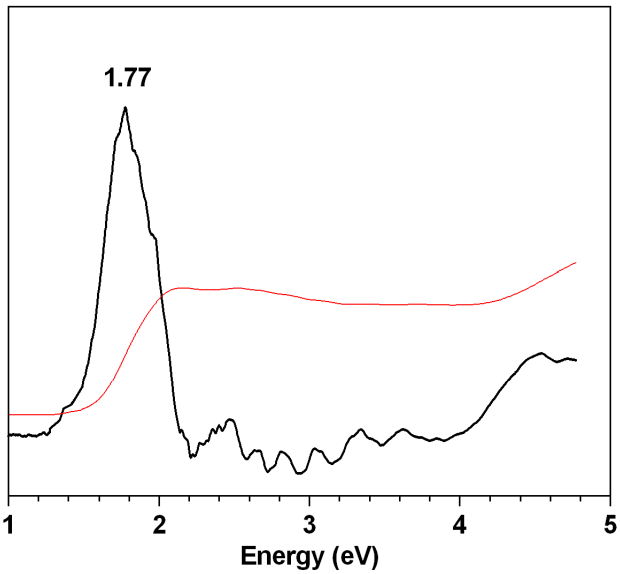

Figure S18. The Kubelka-Munk equation transformed UV-Vis absorption of **1⊃DMF** (red line). The first derivative of the absorption spectrum equation was calculated (black line), and the inversion points were identified as 1.77 eV.

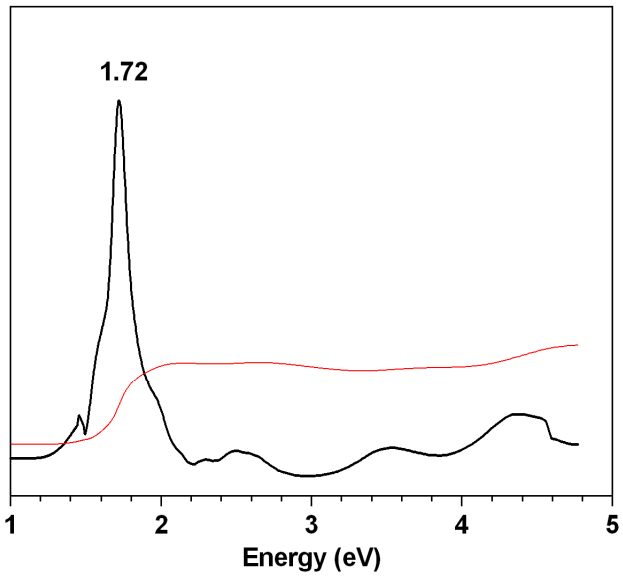

Figure S19. The Kubelka-Munk equation transformed UV-Vis absorption of **1⊃Acetone** (red line). The first derivative of the absorption spectrum equation was calculated (black line), and the inversion points were identified as 1.72 eV.

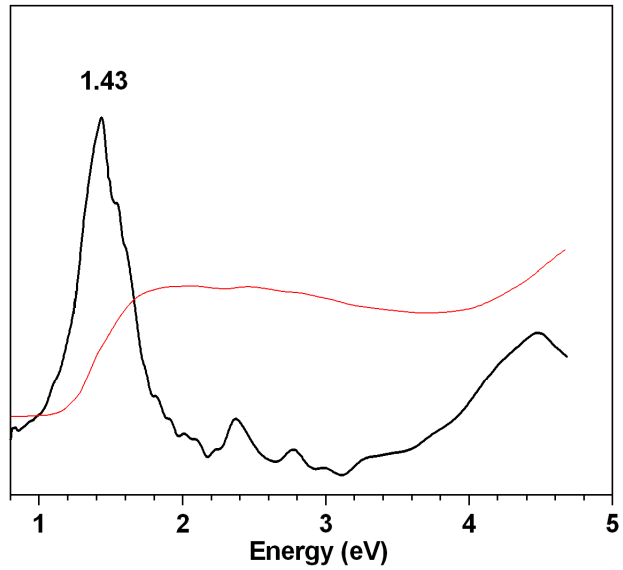

Figure S20. The Kubelka-Munk equation transformed UV-Vis absorption of **1⊃$CHCl_3$** (red line). The first derivative of the absorption spectrum equation was calculated (black line), and the inversion points were identified as 1.43 eV.

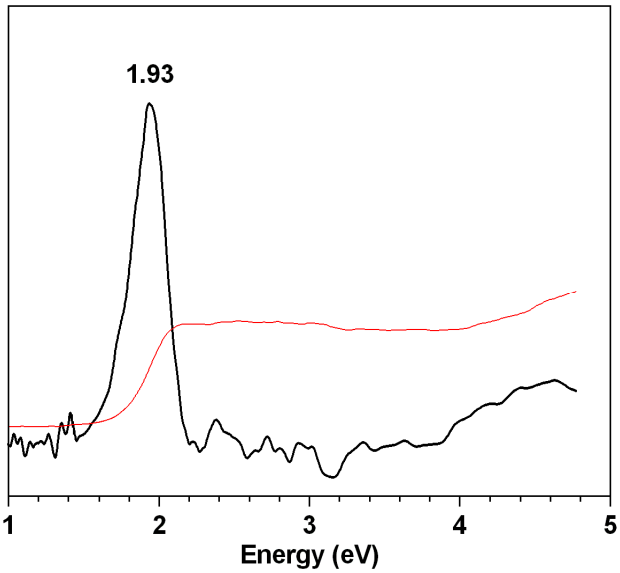

Figure S21. The Kubelka-Munk equation transformed UV-Vis absorption of **1⊃H_2O** (red line). The first derivative of the absorption spectrum equation was calculated (black line), and the inversion points were identified as 1.93 eV.

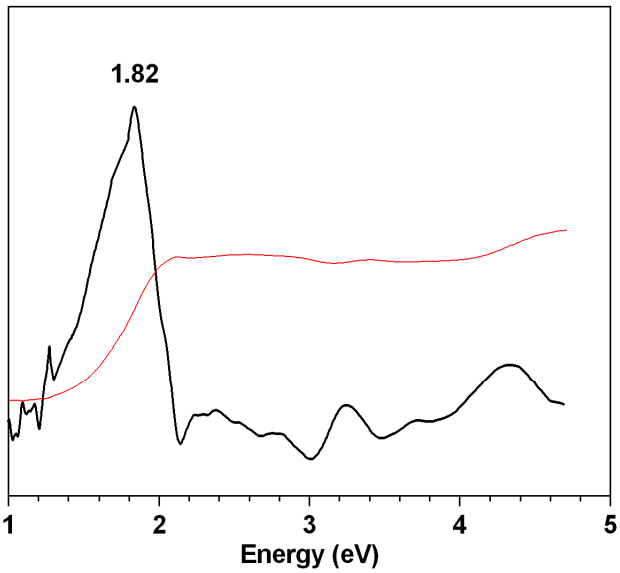

Figure S22. The Kubelka-Munk equation transformed UV-Vis absorption of **1⊃CH_3OH** (red line). The first derivative of the absorption spectrum equation was calculated (black line), and the inversion points were identified as 1.82 eV.

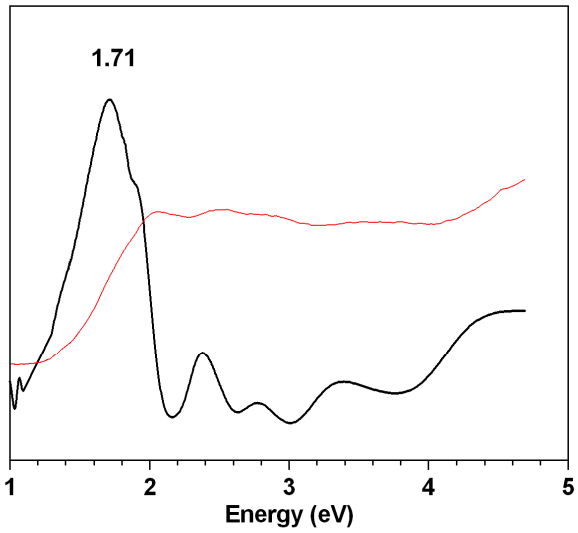

Figure S23. The Kubelka-Munk equation transformed UV-Vis absorption of **1**⊃C_2H_5OH (red line). The first derivative of the absorption spectrum equation was calculated (black line), and the inversion points were identified as 1.71 eV.

5. Supporting figure, PXRD, UV-vis, IR and photograph for 2

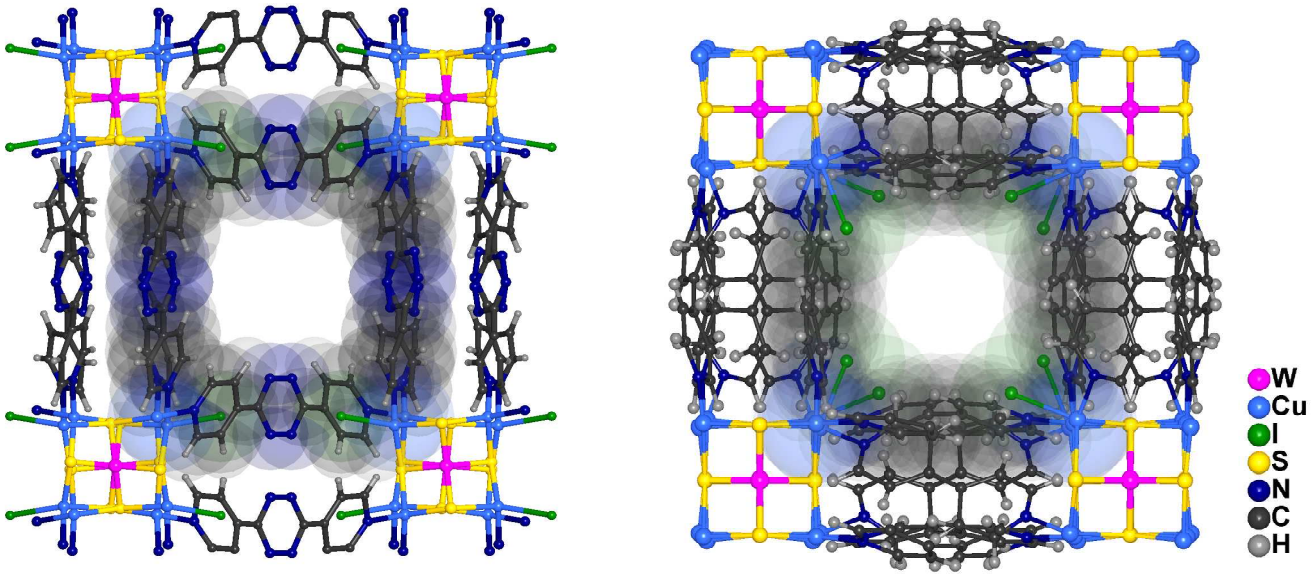

Figure S24. Nanotube of of **1** (left) and **2** (right). The semi-transparent region showing the van der Waals radii of atoms in the inner-surface.

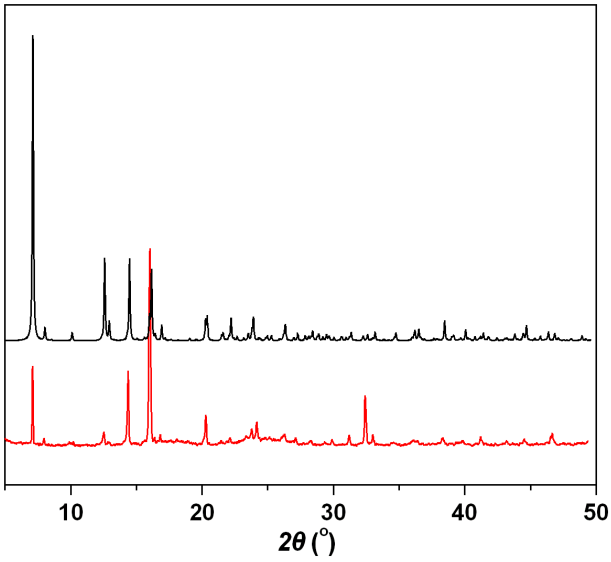

Figure S27. PXRD of stimulated **2**⊃DMF (black) and as-made **2**⊃DMF (red).

Figure S25. Photographs of different inclusion compound of **2**⊃solvent, the included solvents are CH_3CN, H_2O, CH_3OH, DMF, Acetone, C_2H_5OH and CH_3Cl form left to right.

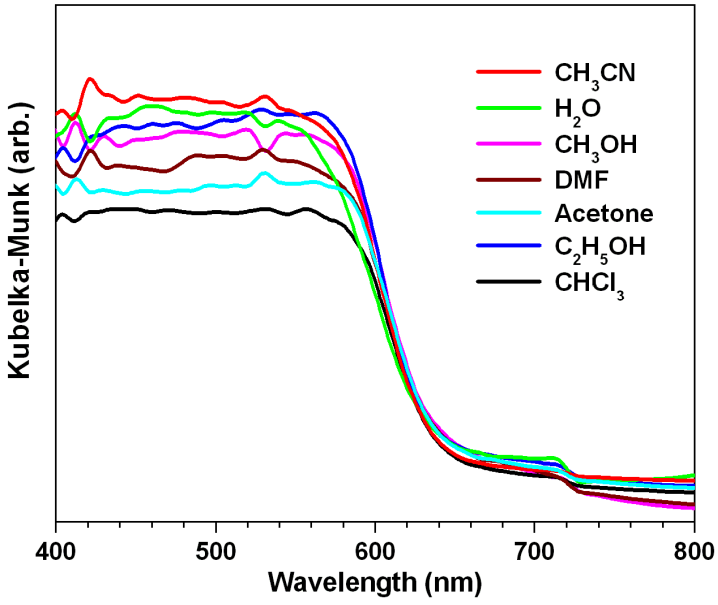

Figure S26. The UV-vis spectra of different solvent inclusion compounds of **2**⊃solvent.

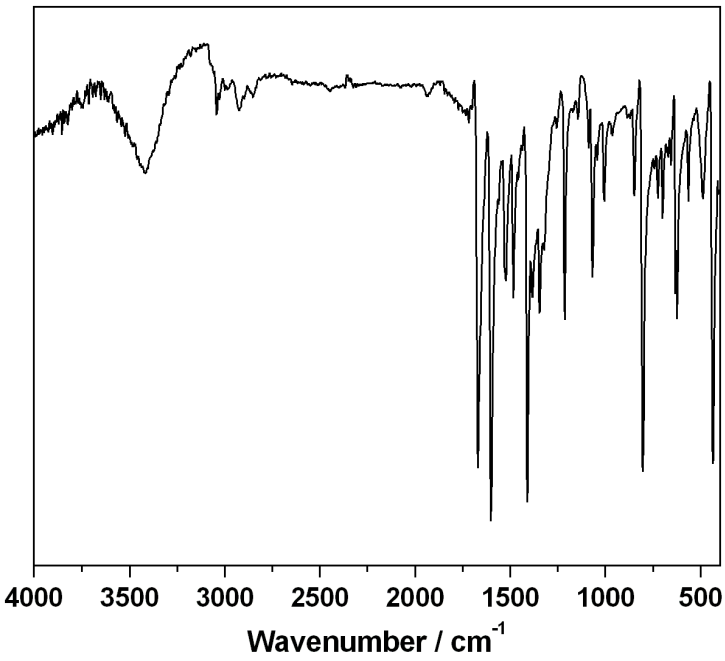

Figure S28. IR spectra of as-made sample **2⊃DMF**

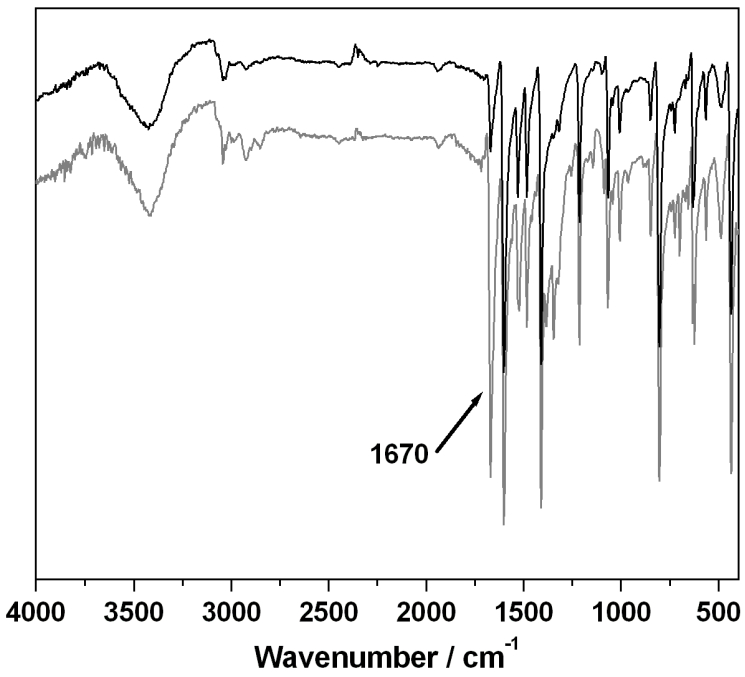

Figure S29. IR spectra of **2⊃CH_3CN** (black) and **1**⊃DMF (gray), the sharply decrease of the strong peak at 1670 (the C=O stretching peak of DMF) indicates the exchanging of DMF with CH_3CN.

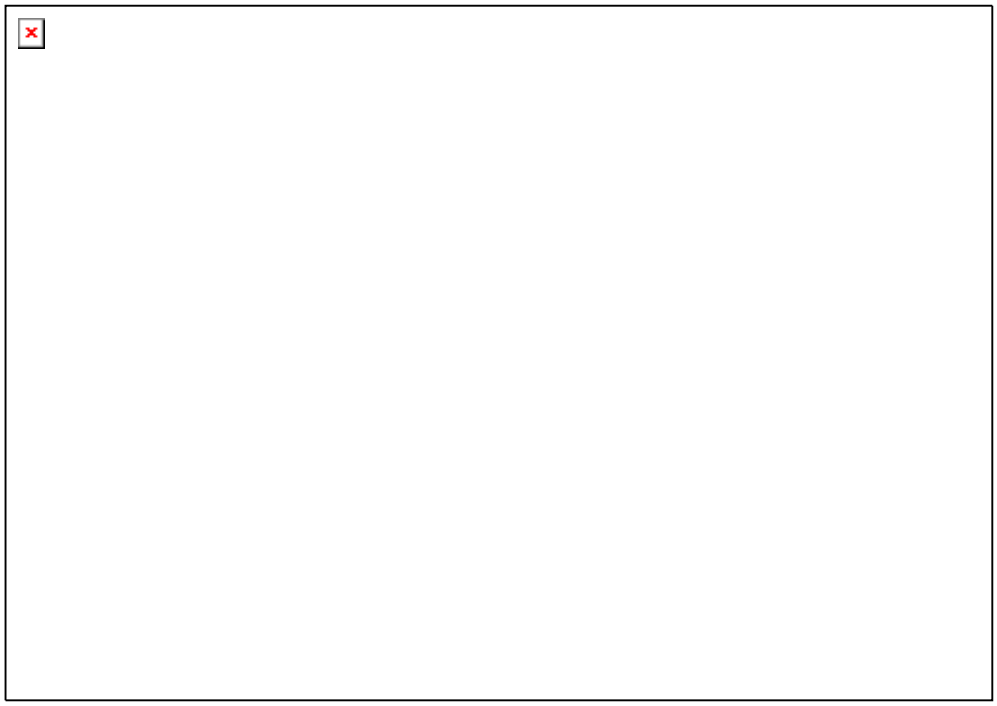

Figure S30. IR spectra of **2⊃Acetone** (black) and **1**⊃DMF (gray), the sharply decrease of the strong peak at 1670 (the C=O stretching peak of DMF) and the appearance of peak at 1710 (the C=O stretching peak of acetone) indicates the exchanging of DMF with acetone.

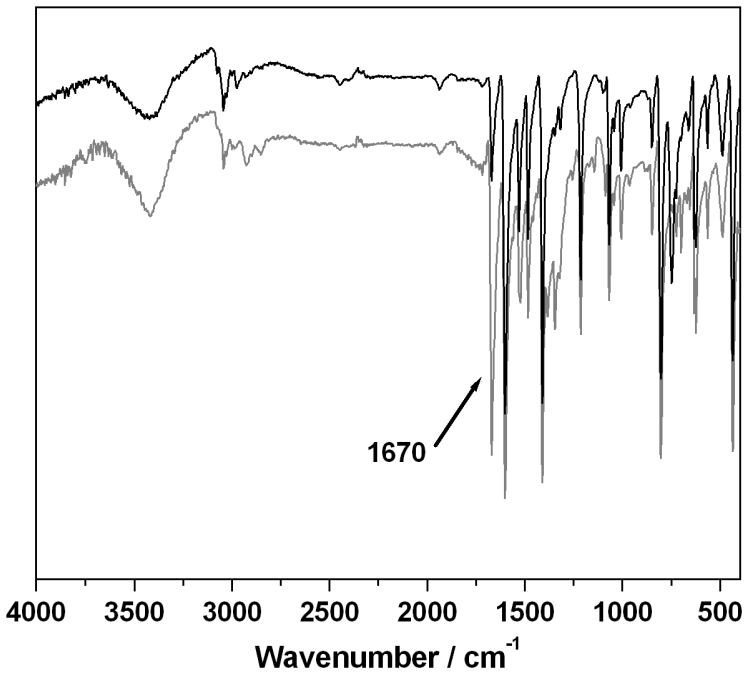

Figure S31. IR spectra of **2⊃$CHCl_3$** (black) and **1**⊃DMF (gray), the sharply decrease of the strong peak at 1670 (the C=O stretching peak of DMF) indicates the exchanging of DMF with $CHCl_3$.

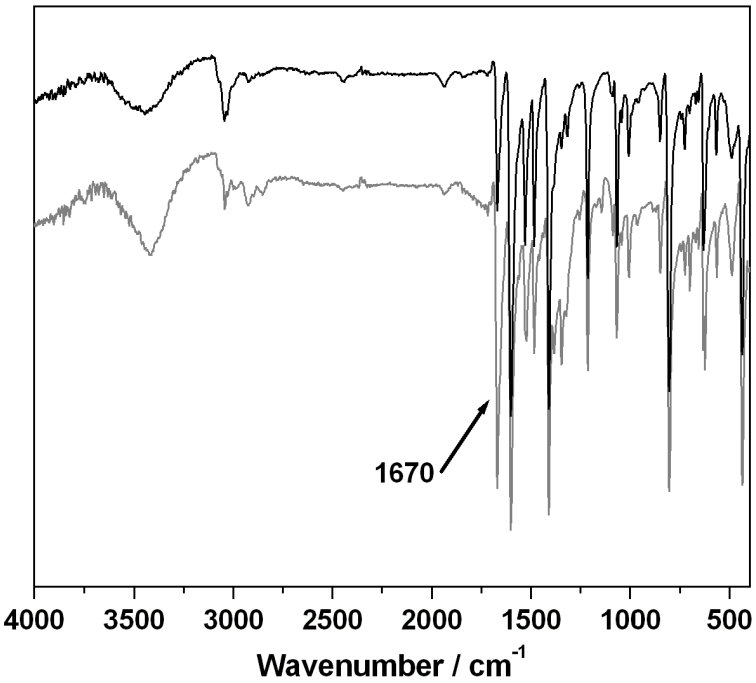

Figure S32. IR spectra of **2⊃H_2O** (black) and **1**⊃DMF (gray), the sharply decrease of the strong peak at 1670 (the C=O stretching peak of DMF) indicates the exchanging of DMF with H_2O.

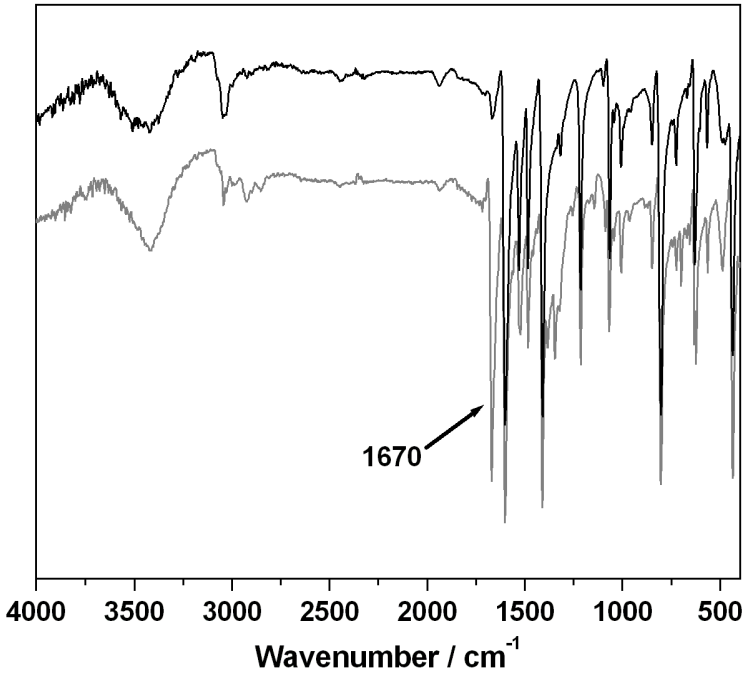

Figure S33. IR spectra of **2⊃CH_3OH** (black) and **1**⊃DMF (gray), the sharply decrease of the strong peak at 1670 (the C=O stretching peak of DMF) indicates the exchanging of DMF with CH_3OH.

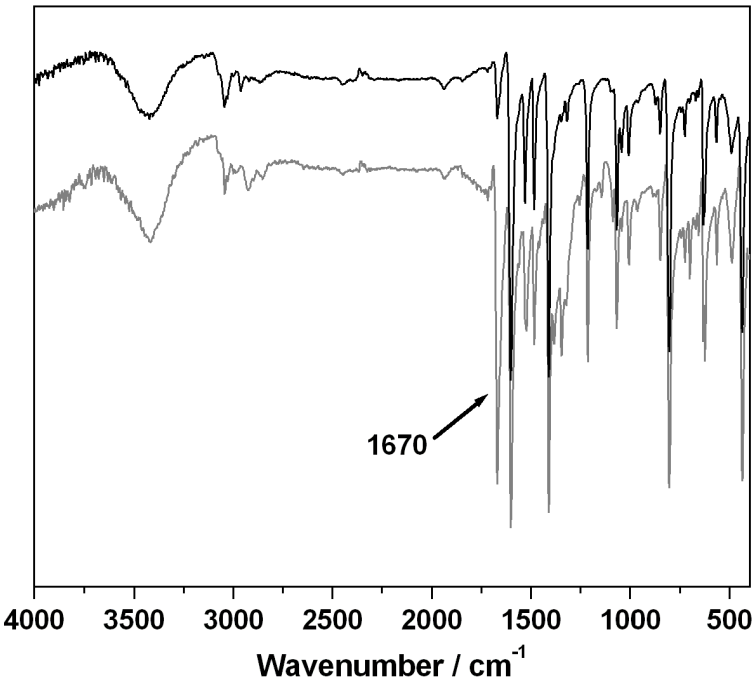

Figure S34. IR spectra of **2⊃C_2H_5OH** (black) and **1**⊃DMF (gray), the sharply decrease of the strong peak at 1670 (the C=O stretching peak of DMF) indicates the exchanging of DMF with C_2H_5OH.

6. References

[S1] Ligand dptz: Bentiss, F.; Lagrenée, M.; Traisnel, M.; Mernari, B.; Elattari, H. *J. Heterocyclic Chem.***1999**, *36*, 149. $(NH_4)_2WS_4$: McDonald, J. M.; Friesen, G. D.; Rosenhein, L. D.; Newton, W. E. *Inorg. Chim. Acta* **1983**, *72*, 205.

[S2] SAINT+, version 6.22; Bruker Analytical X-ray Systems, Madison, WI, **2001**.

[S3] Spek, A. L. *J. Appl. Crystallogr.* **2003**, *36*, 7.

[S4] Gascon, J.; Hernández-Alonso, M. D.; Almeida, A. R.; van Klink, G. P. M.; Kapteijn, F.; Mul, G. *ChemSusChem* **2008**, *1*, 981.